Asociación Argentina
de Mecánica Computacional

Mecánica Computacional Vol XXVIII, págs. 381-391 (artículo completo)
Cristian García Bauza, Pablo Lotito, Lisandro Parente, Marcelo Vénere (Eds.)
Tandil, Argentina, 3-6 Noviembre 2009

MODELING OF WATERHAMMER EVENTS USING A LAGRANGEAN FORMULATION

Hugo Ballesteros[a], **Julián Di Cesare**[a], **Luis Lencina**[a] **and Eduardo N. Dvorkin**[b]

[a] *Nucleoeléctrica Argentina S.A., Central Nuclear Atucha II, Lima, Prov. de Buenos Aires, Argentina,*
http://www.na-sa.com.ar
[b]*SIM&TEC S.A., Ac. Pueyrredón 2130 5to A, C1119ACR, Buenos Aires, Argentina,*
http://www.simytec.com.ar

Keywords: Waterhammer, pressure waves, finite elements, Lagrangean formulation

Abstract. In this paper we develop a Lagrangean finite element model for simulating waterhammer events in pipes; our finite element model includes the capability to consider different non-miscible fluids (liquids and gases), naturally conserving the mass of the different components and continuously distinguishing the interface between them. It is also possible to include in the model changes in the pipeline section (expansions and contractions).We also consider the interaction between the fluid and the supporting structure.

1 INTRODUCTION

The generation of pressure waves in pipes containing fluids and/or gases is a topic that is frequently encountered in the design of industrial installations. We name as *waterhammer* (Parmakian, 1963; Streeter, 1998) the dangerous pressure build-up that is due to the rapid opening or closing of valves; hence, the pipes and valves have to be designed with enough strength to resist the maximum fluid pressure induced by this phenomenon. In other cases the waterhammer is controlled and used for the rapid activation of security devices.

In any case, in order to have the required insight on the possible activation of waterhammer events and on its consequences, it is necessary to use a computational tool able to reliably model the phenomenon, predict the loads acting on the pipeline components and supporting structure and provide information on the effect of the different design parameters.

In this paper we present a new finite element model for simulating waterhammer problems. We develop a dynamic model of the fluid contained inside the pipes using a Lagrangean description of motion (Dvorkin and Goldschmit, 2005) and we also consider the interaction between the fluid pressure waves and the supporting structure. Our finite element model includes the capability to consider different non-miscible fluids (liquids and gases), naturally conserving the mass of the different components and continuously distinguishing the interface between them. It is also possible to include in the model changes in the pipeline section (expansions and contractions).

The friction between the fluids and the pipes is modeled considering a static and a dynamic component. This is necessary because we need to model very short time intervals where the consideration of fully developed flows is not possible. For the case of only one fluid we validate our results using experimental results obtained from the literature (Marcinkiewicz et al., 2008; Vardy and Brown, 2003; Vardy and Brown, 2004). For the case of non-miscible fluids we verify our results showing that they converge when the analysis meshes are refined.

In our model we use explicit time integration and in each step we recalculate the value of Δt to produce stable and accurate results.

In comparison with the more traditional method of characteristics (Parmakian, 1963), where an Eulerian description of motion is used, the present formulation allows for the consideration of several non-miscible fluids.

2 THE FLUID MODEL

2.1 Fluid elements and constitutive equations

The finite element model of the fluid (liquid or gas) inside a pipe is developed with 1D elements as shown in Fig. 1; a ram flow is assumed and at each node we have only one displacement d.o.f.

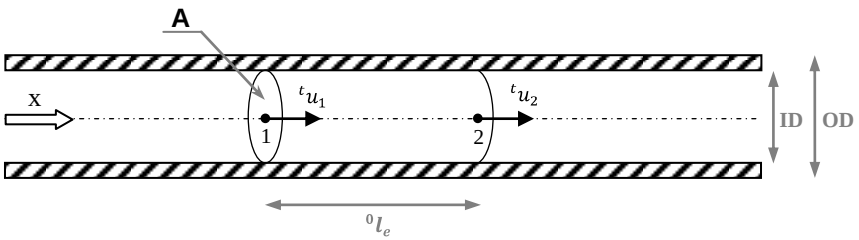

Figure 1: The fluid element

At a time *"t"* the pressure inside the element is calculated using the constitutive equations shown in Table 1 where ${}^{t}V$ and ${}^{0}V$ are the element volume at times *"t"* and *"0"* respectively,

Liquid alt. 1	${}^{t}p - {}^{0}p = -\kappa \ln\left(\frac{{}^{t}V}{{}^{0}V}\right)$
Liquid alt. 2	${}^{t}p - {}^{0}p = -\kappa \frac{{}^{t}V - {}^{0}V}{{}^{0}V}$
Gas	${}^{t}p = {}^{o}p \left(\frac{{}^{t}V}{{}^{o}V}\right)^{\gamma}$

Table 1: Constitutive equations used in the model

For different fluids, the values of κ and γ are obtained from the technical literature.

The position of the nodes inside the piping system is tracked and the fluid volumes at times *"t"* and *"0"* are calculated taking into account the location of each node at the corresponding time: either in a cylindrical zone or in an expansion or in a contraction.

2.2 Time integration

For the time integration of the fluid equilibrium equations we use the explicit time stepping algorithm in Eqn. 1.

For the equilibrium at time *"t+Δt"* we use,

$$
\begin{aligned}
{}^{t+\Delta t}\underline{U} &= {}^{t}\underline{U} + \Delta t\ {}^{t}\dot{\underline{U}} + \frac{1}{2}(\Delta t)^2\ {}^{t}\ddot{\underline{U}} \\
\underline{M}\,{}^{t+\Delta t}\ddot{\underline{U}} &= {}^{t+\Delta t}\underline{R} - {}^{t+\Delta t}\underline{F}({}^{t+\Delta t}\underline{U}) \\
{}^{t+\Delta t}\dot{\underline{U}} &= {}^{t}\dot{\underline{U}} + \frac{\Delta t}{2}\left({}^{t}\ddot{\underline{U}} + {}^{t+\Delta t}\ddot{\underline{U}}\right)
\end{aligned}
\qquad (1)
$$

In the above equations,

${}^{\tau}\underline{U}$, ${}^{\tau}\dot{\underline{U}}$ and ${}^{\tau}\ddot{\underline{U}}$ are the nodal displacements, velocities and accelerations at time τ;

$\underline{M}$ is the mass matrix which, as it is normally done in explicit methods, is a lumped mass matrix;

${}^{\tau}\underline{R}$ is the nodal vector of external forces acting at time τ which includes the friction forces to be discussed in the next subsection;

${}^{\tau}\underline{F}\left({}^{\tau}\underline{U}\right)$ is the nodal vector of internal forces equivalent to the elements pressure, function of the displacements at time τ.

In the step $t \longrightarrow (t + \Delta t)$ we need to fulfill the stability condition (Bathe, 1996),

$$\Delta t \leq \frac{{}^{t}l}{{}^{t}c} \qquad (2)$$

where ${}^{t}c$ is the waves propagation speed at time t. Since both terms on the r.h.s. of Eqn. 2 are

function of time and are also different for each element in the model, the value of Δt is updated for each time step calculating for each element the value that satisfies the equality and then selecting the minimum one.

Considering the circumferential flexibility of a pipe with initial mid-radius "${}^{o}D$", wall thickness *"e"* (assumed constant) and Young modulus *"E"* we calculate at every node,

$$ {}^{t+\Delta t}D = {}^{o}D\left[1 + \frac{2\ {}^{t}F}{\pi\ {}^{t}D\ e\ E}\right] \tag{3}$$

and we use the above diameter in the $t+\Delta t$ equilibrium equations.

2.3 Friction fluid / pipes

2.3.1. Static friction

These models are based on the assumption of fully developed flows which is not applicable for modeling waterhammer events.

For the shear stresses on the wall the static friction model uses the Darcy-Weisbach formula (Streeter et al., 1998),

$$ {}^{t}\tau = \frac{f_q}{8}\ {}^{t}\rho\ {}^{t}\underline{\dot{u}}\ \|\ {}^{t}\underline{\dot{u}}\| \tag{4}$$

where ${}^{t}\rho$ is the fluid density and ${}^{t}\underline{\dot{u}}$ is the fluid velocity. The coefficient f_q is obtained as a function of the flow *Re*, the wall asperity and the pipe diameter (Streeter et al., 1998).

2.3.2. Dynamic friction

The available dynamic friction models can be classified in two groups:

- The models where the shear stresses are calculated as a function of the actual flow conditions; e.g. the Brunone model (Marcinkiewicz et al., 2008)
- The models where the shear stresses are calculated as a function of the flow history; e.g. the Vardy-Brown model (Vardy and Brown, 2003; Vardy and Brown, 2004).

The Brunone model

The Brunone model uses,

$$ {}^{t}\tau = \frac{k_3\ {}^{t}\rho\ {}^{t}D}{4}\left(\frac{\partial \dot{u}}{\partial t} + {}^{t}c\ sign(\dot{u})\frac{\partial \dot{u}}{\partial x}\right) \tag{5}$$

where ${}^{t}D$ is the inner pipe diameter and,

$$ k_3 = \frac{\sqrt{C^*}}{2}; \qquad C^* = \frac{12.86}{Re^{\kappa}} \quad \text{and} \quad \kappa = log_{10}\left(\frac{15.29}{Re^{0.0567}}\right)$$

If Re<2320 use in the above Re=2320.

The Vardy-Brown model

The Vardy-Brown model uses,

$$^{t}\tau = \frac{4\mu}{D}\int_0^t \frac{\partial \dot{u}}{\partial t}(\xi)W(t-\xi)d\xi \tag{6}$$

where μ is the fluid dynamic viscosity and,

$$W(\tau) = \frac{A^* e^{-\tau/c^*}}{\sqrt{\tau}}$$

$$\tau = \frac{4\nu t}{D^2}$$

$$A^* = \frac{1}{2\sqrt{\pi}}$$

In the above equation ν is the kinematic viscosity.
The Vardy-Brown model is computationally more expensive than the Brunone model.

3 FLUID-STRUCTURE INTERACTION

3.1 Fluid loads on the structure

The fluid introduces loads on the structural components due to the action of the internal/external pressure on the curved pipes (Dvorkin and Toscano, 2001), as it is shown in Fig. 2.

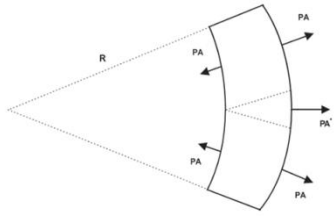

Figure 2: Loads due to the action of the internal/external pressure on curved pipes

Using the principle of momentum conservation in Fig. 3 we get,

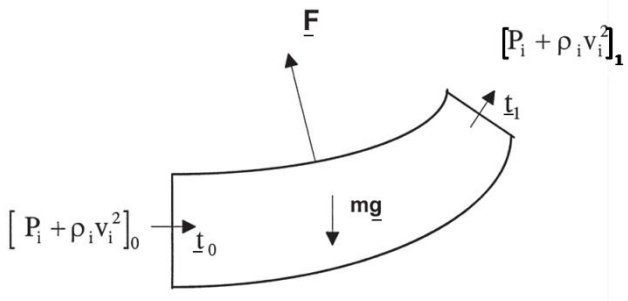

Figure 3: Momentum conservation in a curved pipe

$$\underline{F} = m\underline{g} + [p_i A_i + \rho_i \dot{u}_i]_0 \underline{t}_0 - [p_i A_i + \rho_i \dot{u}_i]_1 \underline{t}_1 \tag{7}$$

In the above equation $\underline{F}$ is the load that the structure inputs on the fluid (the load that the

fluid inputs on the structure is $-\underline{F}$) and m is the mass of the fluid inside the pipe section.

3.2 Solution technique for the FSI

The displacements, velocities and accelerations calculated using Eqns. 1 are referred to a coordinate system that moves together with the pipes (non-inertial coordinate system)

To couple the dynamic behavior of the fluid with the dynamic behavior of the structure we go through the following sequence:

- We know at time *"t"* the displacements velocities and accelerations of the nodes in the fluid model $({}^{t}\underline{U}, {}^{t}\underline{\dot{U}}, {}^{t}\underline{\ddot{U}})_{\text{fluid}}$ and of the nodes in the structural model $({}^{t}\underline{U}, {}^{t}\underline{\dot{U}}, {}^{t}\underline{\ddot{U}})_{\text{structure}}$.
- Mapping the fluid nodes on the structural model we transfer the loads (friction + pressure loads) that the fluid imposes on the structure.
- We solve for the $({}^{t+\Delta t}\underline{U}, {}^{t+\Delta t}\underline{\dot{U}}, {}^{t+\Delta t}\underline{\ddot{U}})_{\text{structure}}$ using also an explicit time stepping algorithm.
- We input on each fluid model node *"k"* the inertia forces ${}^{t+\Delta t}\underline{R}^{k}_{inertia} = -m_k \, {}^{t+\Delta t}\ddot{u}^{k}_{structure} \, \underline{t}^{k}$; where m_k the fluid mass that is lumped at node *"k"* and $\underline{t}^{k}$ is the pipe direction.
- Using the loads previously discussed and the above mentioned inertia forces we solve for $({}^{t+\Delta t}\underline{U}, {}^{t+\Delta t}\underline{\dot{U}}, {}^{t+\Delta t}\underline{\ddot{U}})_{\text{fluid}}$

4 NUMERICAL EXAMPLES

In the problems that follow we model the opening and closing of valves, it is important to notice that:

- When the valve operation time tends to zero the numerical results become quite noisy; however, very good results are obtained for actual valve operational times (in the order of 1/100 sec). A cosine function is used to simulate the opening of the valve.
- In our Lagrangean model the valve has to be modeled attached to a node rather than to a point fixed in space.

The steel Young modulus was considered in the examples that follow

4.1 Validation of the friction models implementation

The experimental results were published in (Marcinkiewicz et al., 2008). The analyzed case is depicted in Fig. 4.

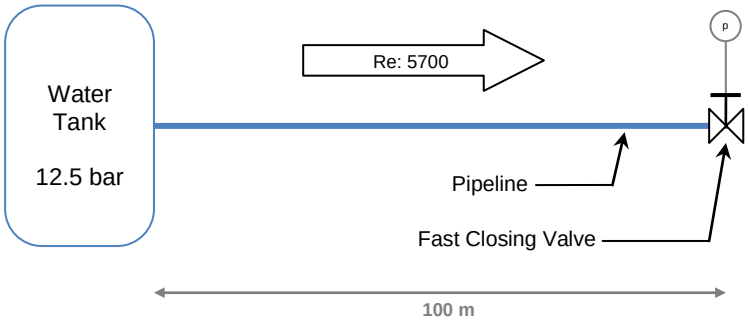

Figure 4: Waterhammer experiment. The valve is closed at t=0; the pipe dimensions are L=100m; ID=0.016m and OD=0.018m. Fluid: water (blue)

In the following figures where we analyze the model results we use,

$$H^* = \frac{\Delta p}{\rho + 2\, c\, V_0} \qquad t^* = \frac{t\, c}{L}$$

The comparison between the experimental results and our numerical results obtained using 100 elements is presented in Fig. 5.

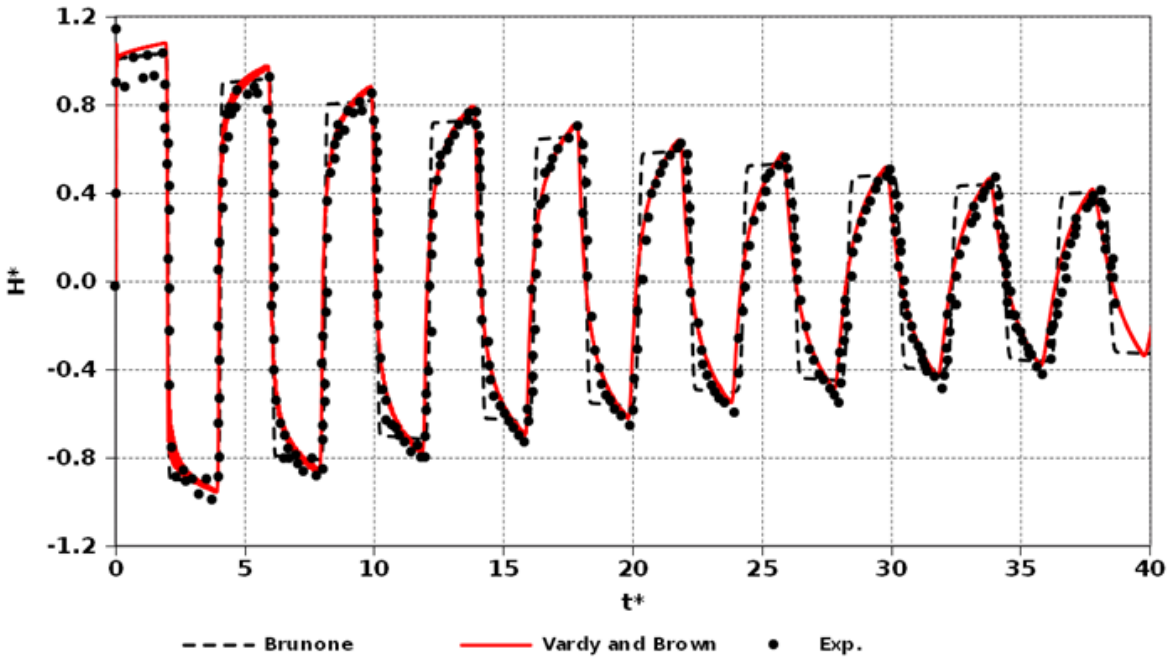

Figure 5: Normalized pressure at the valve. Comparison of calculated and experimental results

For both models the agreement between the numerical results and the experimental data is excellent; however the Vardy-Brown model provides better results.

In Fig. 6 and Fig. 7 we compare for the Brunone and Vardy-Brown models the results obtained using our finite element model and the method of characteristics (MOC)

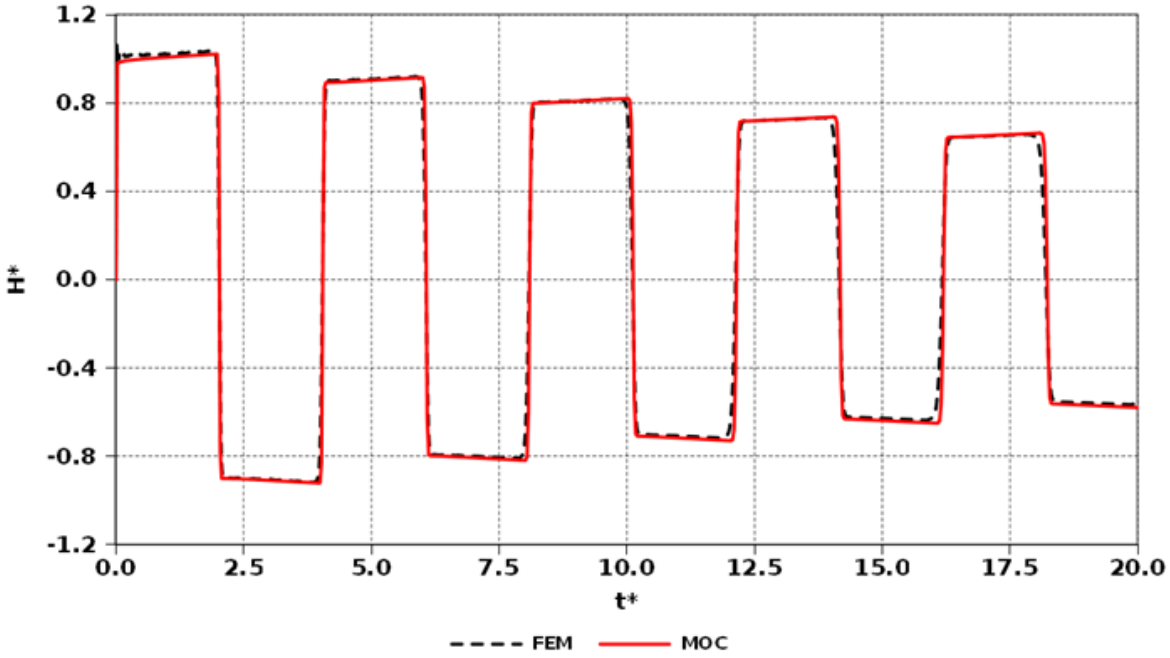

Figure 6: Normalized pressure at the valve. Comparison of Brunone model calculated with FEM and MOC formulations

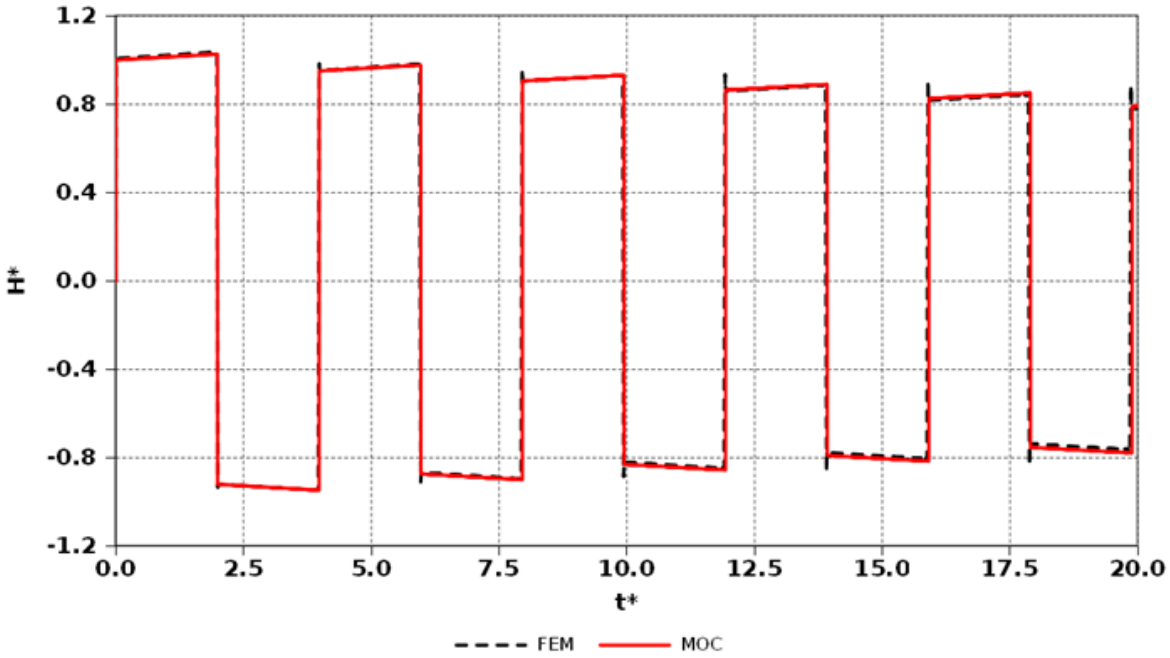

Figure 7: Normalized pressure at the valve. Comparison of Vardy-Brown friction model calculated with FEM and MOC formulations

In this case with only one fluid, the results obtained with our finite element model and with the MOC are coincident for both friction models.

4.2 Modeling non-miscible fluids

In Fig. 8 we present the physical problem to be analyzed.

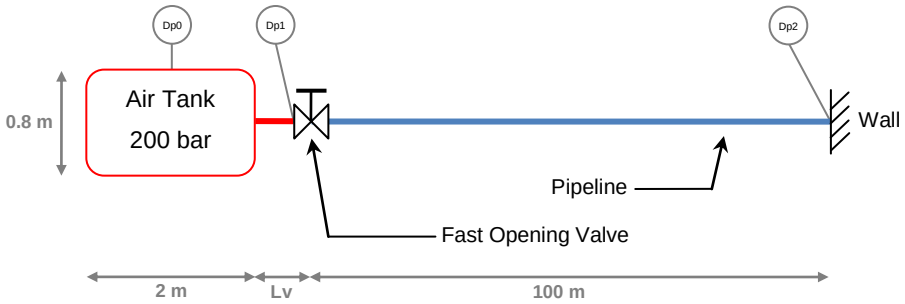

Figure 8: Non-miscible fluids test. The valve is opened at t=0.02; the water pipeline dimensions are L=100m; ID=0.0893m and OD=0.01143m. Fluid: air (red), water (blue)

In Fig. 9 we show how the finite element model converges when we refine the water line mesh.

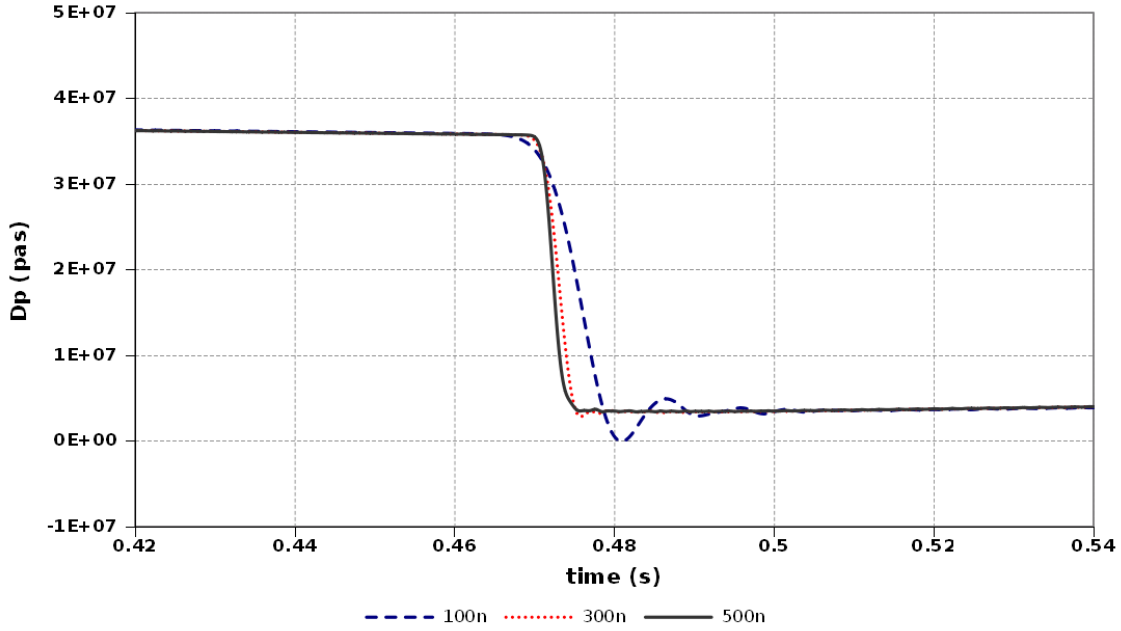

Figure 9: Water line mesh refinement results for Dp2 (we use 13 nodes to model the air and Lv=0)

In Fig. 10 to Fig. 12 we show the convergence when the air section of the model is refined.

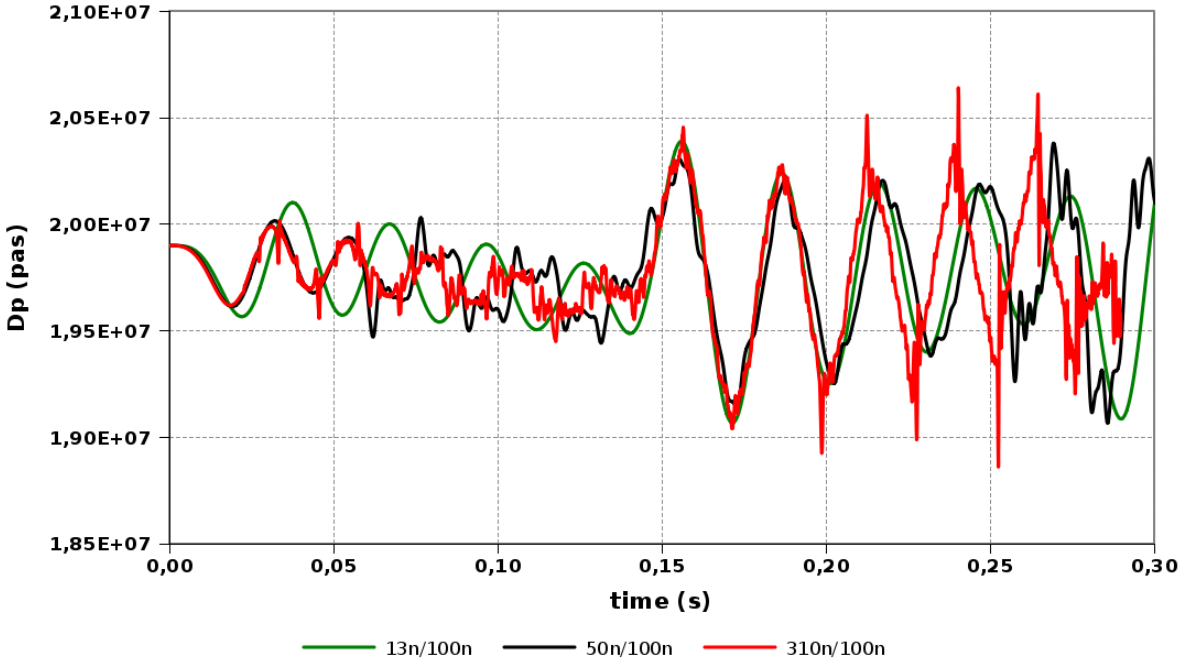

Figure 10: Air mesh refinement results for Dp0

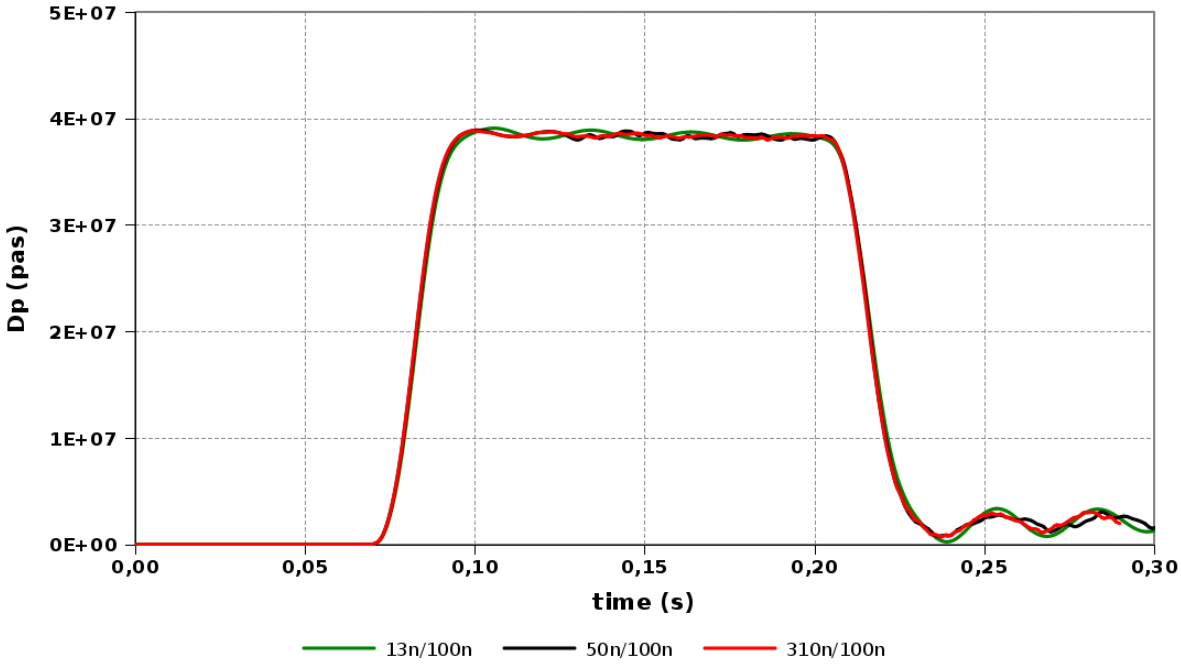

Figure 11: Air mesh refinement results for Dp2

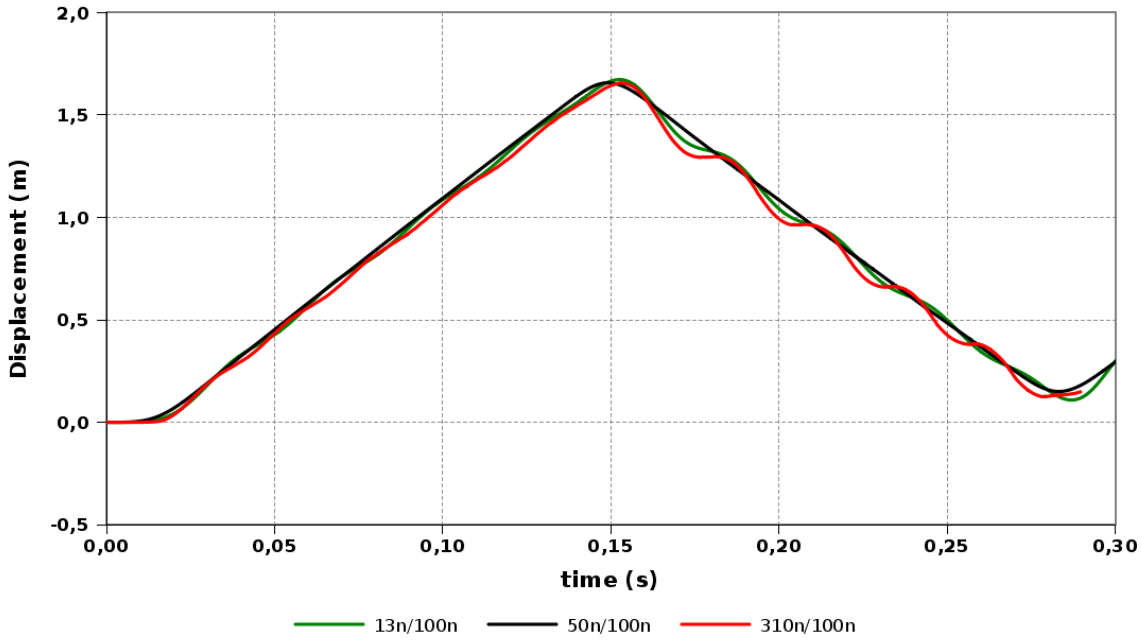

Figure 12: Air mesh refinement results for the interface position

We see from the above results that our model provides convergent results.

It is important to notice that the air elements are quite short and, in accordance, the time steps need to be quite small to fulfill the stability condition in Eqn. 2.

5 CONCLUSIONS

In this paper we developed a Lagrangian finite element model for simulating waterhammer events. The motivation for using a Lagrangian formulation was to include the capability to model the behavior of pipes containing non-miscible fluids.

For the case of only one fluid (water) we have validated our finite element model comparing its results with experimental results.

For the case of non-miscible fluids we have verified the model showing that it converges when the analysis meshes are refined.

In a forthcoming paper we are going to present the verification of the model for cases in which the FSI is considered and expansions / contractions are included in the pipeline.

REFERENCES

Bathe, K.J. *Finite Element Procedures*, Prentice Hall, 1996.

Dvorkin, E.N. and Goldschmit, M.B., Nonlinear Continua, Springer, Berlin, 2005

Dvorkin, E.N. and Toscano, R.G., Effects of external/internal pressure on the global buckling of pipelines, *Computational Fluid and Solid Mechanics – Proceedings First MIT Conference on Computational Fluid and Solid Mechanics*, (Ed. K.-J.Bathe), Elsevier, 2001.

Marcinkiewicz, J., Adamowski, A. and Lewandowski, M. Experimental evaluation of ability of Relap5, Drako, Flowmaster and program using unsteady wall friction model to calculate water hammer loadings on pipelines. *Nuclear Eng. and Design*, 239:2084-2093, 2008.

Parmakian J. *Waterhammer Analysis*. Dover, 1963.

Streeter, V.L., Wylie, E.B and K.W. Bedford. *Fluid Mechanics*, McGraw-Hill, 1998.

Vardy, A.E. and Brown, J.M.B. Transient turbulent friction in smooth pipe flows. *J. Sound Vibration*. 259:1011-1036, 2003.

Vardy, A.E. and Brown, J.M.B. Transient turbulent friction in fully rough pipe flows. *J. Sound Vibration*. 270:233-257, 2004.